Master Thesis College of Human Ecology

Influence of Nonwoven Wettability and Pore Characteristics on Bacterial Adhesion

부직포의 젖음성과 기공 특성이 박테리아 부착성에 미치는 영향

August 2021

Graduate School of Seoul National University
Department of Textiles, Merchandising, and Fashion Design

HEMMATIAN TAHMINEH
하나

Influence of Nonwoven Wettability and Pore Characteristics on Bacterial Adhesion

지도교수 김주연

이 논문을 의류학석사 학위논문으로 제출함
2021년 8월

서울대학교 대학원
의류학과
HEMMATIAN TAHMINEH(하나)

하나의 의류학석사 학위논문을 인준함
2021년 8월

위 원 장 _____

부 위 원 장 _____

위 원 _____

ABSTRACT

Textiles can act as a media to deliver pathogenic organisms and spread infectious diseases. For controlling bacterial adhesion on surfaces, it is crucial to understand the substrate characteristics and how bacteria interact with substrates. For an accurate evaluation of textile-adhered bacteria, a proper evaluation method is necessary, because a complex 3D structure of fibrous material makes quantification of adhered bacteria challenging. Therefore, in the first phase of the study, colorimetric bacteria assay method using the iodonitrotetrazolium (INT) stain was tested for quantifying the textile-adhered bacteria. In the second phase of the study, the textile parameters including wettability, porosity, pore-volume, and pore size distribution were investigated in association with the bacterial adhesion property. Two different types of bacteria, gram-negative rod shape *Escherichia coli* (*E. coli*) and round shape *Staphylococcus aureus* (*S. aureus*) were used as model bacteria. Substrates with different levels of wettability and pore characteristics were employed to identify the critical factors influencing cell adhesion. The substrate's wettability appeared to be the initial factor influencing the bacterial adhesion, where the hydrophilic surface showed considerably higher bacterial adhesion. Substrates with high wettability provided higher contact areas for bacteria to adhere to the

substrates. Pore volume and pore size, rather than the porosity (%) itself, were other important factors affecting bacterial adhesion and retention. Compact spatial distribution of fibers resulted in limited bacterial intrusion into the pores, and eventually reduced the total amount of bacterial adherence. Thus, superhydrophobic textiles with reduced total pore volume and smaller pore size would reduce the adhesion. The findings of this study can be used as a design guide for anti-biofouling textiles.

Keyword: bacterial adhesion; electrospun web; wetting; morphology; pore; plasma treatment; *Staphylococcus aureus; Escherichia coli*

Student ID: 2018-28019

CONTENTS

List of tables

List of figures

Chapter 1. Introduction

1. Background and Objectives

Bacterial adhesion on nonwovens not only increases the risk of cross-contamination but also limits the substrate performance [1-6]. To control bacterial adhesion, it is important to understand substrate characteristics affecting it and interactions between bacterial cells and substrate surface. Nonwoven substrate is porous and rough, and such morphological characteristics make bacterial adhesion more complex [7-9]. There are conflicting findings regarding bacterial adhesion, and little has been examined on the effect of fibrous morphology.

The main objective of this study is to investigate physicochemical characteristics of nonwoven substrates that affect adhesion of bacteria and to suggest design factors of textiles relating to control bacterial adhesion. Specific objectives include developing a relevant analytical method to quantify the number of bacterial cells from nonwoven substrates. Particular interest lies on the role of nonwoven substrate's wettability, porosity percentage, total pore volume, and pore size on interactions of nonwoven with bacterial attachment.

This study is novel in that pore characteristics, which are unique to nonwoven substrates, were considered in interpreting the interaction

between bacterial cells and nonwovens. Earlier studies were focused on surface roughness patterns and wetting properties concerning bacterial adhesion, and little has been discussed on effect of pore characteristics of nonwovens. In this study, bacterial adhesion and its retention inside the substrate volume were examined for explaining the bacterial adhesion on nonwovens. By understanding the fiber substrate characteristics affecting the bacterial adhesion, a proper design of nonwovens could be suggested to circumvent the adherence of infectious bacteria. The results of this study would ultimately contribute to enhancing the hygiene aspect of nonwovens and to reduce the malfunction attributable to bacterial adhesion of substrate.

2. Theoretical Background

2.1. Microbial contamination of nonwoven substrates

Since nonwoven substrates have surface roughness and pores in the volume, they can provide a dynamic environment for bacteria to adhere, grow, and form biofilm which result in bacterial infection and malodor production [10-12]. To prevent this event, antimicrobial treatments are frequently applied using biocidal materials or antibiotics. For example, antimicrobial agents such as quaternary ammonium compounds and triclosan were incorporated into fibers [13].

Among the biocidal nanoparticles, silver [14-16], copper [16,17], titanium dioxide [18-20], and zinc oxide [21,22] are frequently used in a wide range of materials due to their efficacy at killing bacteria through interacting with microbial proteins [15,23-25]. Yet, the influence of nanoparticles and their toxicity on human cells is not fully understood [26-28], and this limits the application of such nanoparticles [29-32].

Antibiotics such as doxymycin, cefadroxil, and ciprofloxacin are also often used to kill the bacteria by targeting cell membrane, DNA, or RNA [33,34]. However, with the evolution of antibiotic-resistant bacteria, concerns about abusive use of antibiotics have been

addressed. Indeed, a growing number of widely used antibiotics are becoming ineffective [35].

Thus, as an alternative approach to control the bacterial growth on nonwovens, modifying the physiochemical properties of nonwovens has been largely explored to resist the bacterial adhesion to surfaces by altering the surface characteristics of nonwoven substrates [36-39]. To this end, multiple physical aspects of substrates have been considered, including surface energy, wettability, and topography.

2.2. Factors affecting bacterial adhesion to substrates

2.2.1. Surface energy

Surface energy of substrate, with its polar and disperse components, is known to be one of the important characteristics of a solid surface that affects bacterial adhesion. Substrate's surface chemistry with its polar and disperse components of surface energy affects surface wettability and bacterial adhesion. The effect of surface energy on bacterial adhesion may differ depending on the bacterial cell characteristics. It was observed that *S. aureus* adhesion increased when the surface energy of a film substrate increased, while *E. coli* adhesion slightly decreased [40].

From the study by Wang *et al.* [41], with the increase in surface

free energy of polyethylene terephthalate (PET) after carbon film deposition, adhesion of *Staphylococcus epidermidis* (*S. epidermidis*) and *S. aureus* decreased. On the other hand, Rochford *et al.* [42] study showed that O_2 plasma modified PEEK surface increased *S. aureus* adhesion.

Triandafillu *et al.* [43] study showed O_2 plasma-treated surface of polyvinyl chloride (PVC) reduced adhesion of *Pseudomonas aeruginosa* (*P. aeruginosa*) by 70%. On the contrary, the same treatment of PET and poly (methylhydrosiloxane) favored *P. aeruginosa* adhesion and biofilm formation. As shown from the previous studies, the results of bacterial adhesion on the substrates with varied surface energies are not consistent, and further investigation on the effect of surface energy on the bacterial adhesion on nonwoven surfaces is needed.

2.2.2. Morphology of nonwoven substrates

The effect of the spatial distribution of roughness patterns on bacterial adhesion has been reported [44]. However, how nano- and micro-scale roughness patterns in nonwoven substrates influence bacterial adhesion could not be generalized, since size and shape of bacteria are also believed to play a role in interactions with substrate surfaces. The complexity also comes from the fact that the roughness

together with surface energy, affects the wetting property [45-47]. When roughness is introduced onto a low surface energy substrate, the wettability of the surface is further reduced, ultimately leading to a superhydrophobic surface.

Yet, additional studies are needed on the spatial distribution of roughness structures and macroscopic/microscopic patterns on fibrous surfaces relative to bacteria size for determining the roughness criteria of geometries and scales that most effectively control the bacterial adhesion. Surface properties of substrates play a critical role in bacteria-surface interactions [48,49]. Although being important, the surface property itself may not give a full understanding of the interaction between bacteria and substrates. Nonwoven substrates contain numerous pores that may act as trap sites for bacteria. Therefore, although considering the pore characteristics and roughness of nonwoven substrates in assessing the bacterial adhesion seems to be essential, those factors rarely have been investigated.

2.2.3. Wettability

Among the parameters affecting bacterial adhesion, wettability which is represented by contact angle (CA) between the solid and liquid, has been considered as the most relevant parameter dictating the microbial adhesion on surfaces [50]. Roughness together with

surface energy affect the wettability characteristic. Previous studies investigated the effect of wettability on bacterial adhesion, while the results are hardly conclusive [51].

Superhydrophobic surfaces with water contact angle more than 150° and a low roll-off angle have been generally reported to be anti-adhesive to bacterial cells by weakening the bacterial adhesion. This phenomenon is called "self-cleaning ability," in which loosely adhered bacteria are detached easily by gentle rinsing. Moderate hydrophobic surfaces often show immense adherence of bacteria, especially for the gram-negative cells with lipopolysaccharide membrane [52]. Bacterial adhesion on hydrophilic surfaces is argumentative; some studies showed an intensified adhesion of bacteria on hydrophilic surfaces, regardless of gram characteristics of cells, and some other studies reported the anti-adhesive properties against cells for hydrophilic surfaces [52-55].

2.3. Quantification methods of bacterial adhesion to substrates

Complex multilayer structure of fibrous substrates makes the quantification of adhered bacteria more challenging. Therefore, since interpretation of bacterial adhesion depends on the evaluation methods, developing an accurate method for nonwoven-adhered bacteria

quantification is a prerequisite for the research.

In previous studies, microscopic analysis has been commonly employed to visually observe the adhered bacteria on surfaces [52,56-60]. However, it is difficult to accurately count the bacteria inside fibrous substrates [52]. Staining may enhance the visibility of bacteria presence, but common dyes may stain not only the bacteria but also the substrate itself, resulting in high background signals [61,62].

Fluorescence labelling of bacteria is a convenient way of visualizing the bacteria [60,63-69], but careful adjustment of light exposure should be made to minimize the influence of auto-fluorescence of polymeric background [52,70]. The extraction method [40,71,72] that releases the adhered bacteria prior to measuring optical density or counting the colony-forming units (CFU) is another commonly applied quantification method but it may lack precision if the bacteria detachment from the surface is incomplete [73,74].

For accurate quantification, metabolic activity of viable bacteria can be detected, but it requires sophisticated techniques and substrates. Recently, optical visualization method using iodonitrotetrazolium (INT) chloride was suggested as a cost-effective quantification method for nonwoven-adhered bacteria, where INT changes color to purple upon capturing two electrons from viable bacteria [61].

Chapter 2. Experiment

1. Materials

Gram-negative strain *Escherichia coli* KCTC 1039 (*E. coli*) received from Korean Collection for Type Cultures (KCTC, Jeollabuk-do, Korea) and gram-positive strain *Staphylococcus aureus* ATCC 6358 (*S. aureus*) obtained from Koram Biotech Corp., (Seoul, Korea) were used as model bacterium. Polylactic acid (PLA) resin (Ingeo 4043D, 98% L-lactide, Mw~111,000) was purchased from NatureWorks (Green Chemical Co., Ltd., Seosan-si, Chungcheongnam-do, Korea). Polystyrene (PS) pellets (Mw~350,000), tetrahydrofuran (THF), dimethylformamide (DMF), dichloromethane (DCM), dimethyl sulfoxide (DMSO), chloroform (CHF), and toluene (TOL) were obtained from Sigma-Aldrich (St. Louis, MO, USA). Phosphate buffered saline (PBS, pH 7.4) and methylene iodide (MI) were purchased from Thermo Fisher Scientific (Fisher Scientific Korea Ltd., Incheon, Korea). Polyethylene terephthalate film (PET-film) was gained from Goodfellow (Jung-gu, Seoul, Korea). Polyethylene terephthalate spunbond (PET-fiber) and polypropylene meltblown (PP-fiber) were supplied from Korea Institute of Industrial Technology (KITECH, Ansan-si, Gyeonggi-do, Korea). Iodonitrotetrazolium chloride (INT) was purchased from TCI chemicals (Tokyo Chemical Industry Co., Ltd.,

Chuo-Ku, Tokyo), culture Luria-Bertani broth (LB) was obtained from ATS Korea (Yongin-si, Gyeonggi-do, Korea).

2. Fabrication of substrates

2.1. Spin coating and electrospinning

Commercially available PET-film, PET-fiber, PP-fiber, and PS-film were used as received. The PLA-film and PS-film were prepared by spin coating (MIDAS spin coater, SPIN-1200D, Daejeon, Korea), 3 mL of 15% (w/v) PLA in CF and 20% (w/v) PS in a 1:1 volume ratio of CHF and TOL. The spinning speed was 500 rpm, and the spinning time was 35 sec.

PLA and PS fibrous webs were prepared by electrospinning (ESR200PR2D, NanoNC, Seoul, Korea). A 10% (w/v) PLA solution with a 1:1 volume ratio of DCM and DMF was electrospun at a feeding rate of 3 $mL.h^{-1}$ at 10 kV. The 22-gauge needle was used, and the tip-to-collector distance was 10 cm. For the PS fiber web, 18% (w/v) PS solution and 25% (w/v) PS solution were prepared in a 1:1 volume ratio of THF and DMF, respectively. An 18% PS solution was electrospun at the feeding rate of 2 $mL.h^{-1}$ and voltage of 22 kV with 12 cm of tip-to-collector distance. A 25% PS solution was electrospun at the feeding rate of 2 $mL.h^{-1}$ and voltage of 13 kV, with the tip-to-collector

distance of 15 cm. For both PS electrospinning a 23-gauge needle was used.

2.2. Surface modification

Surface energies of film and electrospun fibers were modified by plasma treatment, using Covance Plasma System (Femto Science, Hwaseong, Korea). Prior to plasma treatment, all samples were cut to 1 cm × 1 cm sizes, and were cleaned in isopropanol for 5 min using a sonic cleaner (WUC-D03H, Daihan Science Co., Gangwon-do, Korea), then were rinsed with distilled water.

For hydrophilic modification, substrates were treated with oxygen (O_2) plasma at 200 W, 160 sccm for 5 min. Oxygen-treated substrates undergo hydrophilic recovery within a few days of exposure to air; hence O_2 treatments were done right before the bacterial adhesion test. Hydrophobic surface modification was done by the plasma-enhanced chemical vapor deposition (PECVD) using octafluorocyclobutane (C_4F_8). The substrates were subjected to a gas flow of C_4F_8 with 100 sccm for 30 min at 160 W. This procedure was repeated 3 times with 10 min rest between each treatment.

3. Characterization of Substrates

3.1. Substrate's solidity, porosity, and total pore volume

Solidity and porosity of the substrates were calculated using Equations (1) and (2), where m (g) is sample's mass; A (cm^2) is sample's area; t (cm) is sample's thickness; and ρ ($g.cm^{-3}$) is polymer's density (1.21 $g.cm^{-3}$ for PLA; 1.05 $g.cm^{-3}$ for PS). Apparent volume and total pore volume were calculated using Equations (3) and (4).

$$\text{Solidity (unitless)} = m/(A \cdot t \cdot \rho) \quad (1)$$

$$\text{Porosity (\%)} = [1 - m/(A \cdot t \cdot \rho)] \times 100\ (\%) \quad (2)$$

$$\text{Apparent volume } (mm^3) = \text{Surface area} \times t \quad (3)$$

$$\text{Total pore volume } (mm^3) = \text{Apparent volume } (mm^3) \times \text{Porosity} \quad (4)$$

Mean diameter of fibers was obtained by measuring at least twenty fibers from scanning electron microscopy (SEM) images. Pore size distribution of fibers was measured with a capillary flow parameter (CFP-1500AE, Porous Materials Inc., Ithaca, NY, USA). Morphology of the bacteria and substrates was observed by FE-SEM (Supra 55VP, Carl Zeiss, Jena, Germany). Bacterial cells were fixed by osmium tetroxide vapor (2% w/v) for 24 h. Before SEM analysis, all samples were sputter-coated with Pt at 20 mA for 180 s (EM ACE200, Leica, Wetzlar, Germany). In microscopic analysis of the first phase of the

study, adhered bacteria to the substrates were marked using Photoshop CS6. Sample description and characteristics are summarized in Table 1. Number noted next to fibers is the average fiber diameter (μm).

3.2. Wettability

Static contact angle (CA) was measured using contact angle goniometer (Theta Lite, KSV Instruments Ltd., Espoo, Finland). The CA of the liquid drop with volume of 3 μL was measured in 5 s upon deposition on nonwoven substrates or bacteria dried plateau. Mean value of at least 6 measurements was recorded. Bacteria surface was obtained through culturing the cells on an LB agar plate and air-dried for 3 h.

Bacteria surface was obtained by culturing the cells on an LB agar plate and then air-drying for 3 h. Surface energy of each polymeric and bacteria surface with their polar and dispersive components was calculated with Equations (5) – (8) using the CAs of water and methylene iodide and applying the Owens-Wendt model [75]; in which θ (degrees) is CA of liquid on solid and bacteria surface; γ_{SL} (mN/m) is solid/bacteria-liquid interfacial free energy; γ_S (mN/m) is solid/bacteria surface free energy; γ_S^d (mN/m) is solid/bacteria/liquid dispersive component surface free energy; γ_S^p (mN/m) is

solid/bacteria/liquid polar component surface free energy.

$$\gamma_{SL} = \gamma_S + \gamma_L - 2\sqrt{\gamma_S^d . \gamma_L^d} - 2\sqrt{\gamma_S^p . \gamma_L^p} \quad (5)$$

$$\gamma_S = \gamma_{SL} + \gamma_L \cos\theta \quad (6)$$

$$\gamma_L (1 + \cos\theta) = 2\sqrt{\gamma_S^d . \gamma_L^d} + 2\sqrt{\gamma_S^p . \gamma_L^p} \quad (7)$$

$$\gamma_S = \gamma_S^d + \gamma_S^p \quad (8)$$

Table 1. Substrate's description and characteristics.

Code	Description	Thickness (mm)	Basis weight ($g.m^{-2}$)	Solidity (unitless)	Porosity (%)	Mean fiber diameter (mm^3)	Apparent volume (mm^3)	Total pore volume (mm^3)
PLA-film	Polylactic acid film	0.08 (±0.01)	72.6 (±7.7)	1.00	0	NA	9	0
PLA-film(O)	O_2 plasma-treated polylactic acid film							
PLA-film(F)	C_4F_8 plasma-treated polylactic acid film							
PLA-fiber0.8	Polylactic acid fiber	0.15 (±0.02)	19.6 (±4.0)	0.11	89	0.8 (±1.0)	15	1470
PLA-fiber0.8(O)	O_2 plasma-treated polylactic acid fiber							
PLA-fiber0.8(F)	C_4F_8 plasma-treated polylactic acid fiber							
PS-film	Polyester film	0.03 (±0.01)	33.4 (±2.1)	1.00	0	NA	13	0
PS-film(O)	O_2 plasma-treated polyester film							
PS-film(F)	C_4F_8 plasma treated polyester film							
PS-fiber6.8	Polyester fiber	0.09 (±0.00)	11.0 (±1.4)	0.11	89	6.8 (±1.9)	9	801
PS-fiber6.8(O)	O_2 plasma-treated polyester fiber							
PS-film6.8(F)	C_4F_8 plasma treated polyester fiber							
PS-fiber2.2	Polyester fiber	0.34 (±0.05)	17.0 (±5.5)	0.04	96	2.2 (±0.3)	34	3230
PS-fiber2.2(O)	O_2 plasma-treated polyester fiber							
PS-fiber2.2(F)	C_4F_8 plasma treated polyester fiber							

4. Bacterial Adhesion Assay

For quantitative analysis of adhered bacteria, three different methods were tested on PET-film, PET-fiber, and PP-fiber. The methods are as follow: (1) extraction of nonwoven substrates-adhered bacteria, with the subsequent optical density measurement and CFU counting; (2) colorimetric analysis by INT staining of live nonwoven substrates-adhered bacterial cells; and (3) microscopic analysis for calculation of the area fraction covered by bacteria.

4.1. Adhering bacteria to substrates

For bacterial binding to a sample substrate, the substrate was immersed in 1 mL of bacterial culture in LB broth, with the initial OD_{600} of 0.5 that corresponds to ~3.4×10^8 $CFU.mL^{-1}$. The 1 mL of culture and substrate was put in a 24-well plate and incubated for 1 h at 100 rpm. After incubation, the *E. coli*-adhered substrate was placed in a new plate; then, the weakly adhered bacteria were detached from the sample by rinsing the substrate two times in 1 mL PBS at 100 rpm for 5 min. Bacterial binding procedure is illustrated in **Figure 1**.

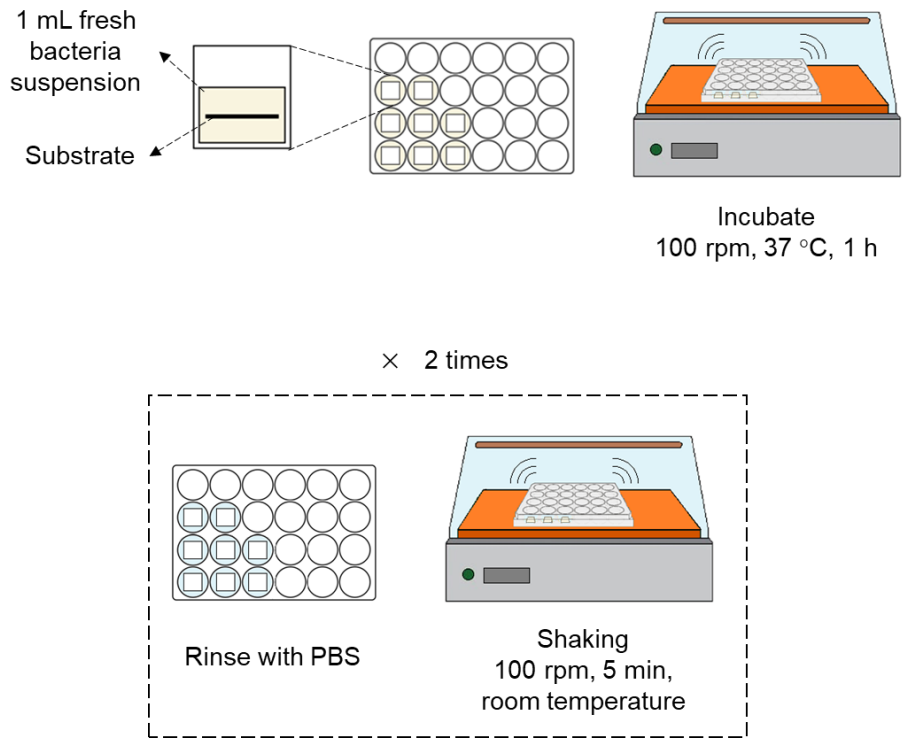

Figure 1. Adhering bacteria to substrates.

4.2. Quantification of adhered bacteria

4.2.1. Method 1: Extraction method

Standard curve for optical density and cell counting. *E. coli* in LB broth was incubated at 37 °C and 200 rpm for 4 h; then the bacteria suspension was pelleted by centrifuging at 3000 rpm for 5 min at 4 °C (MultiCentrifuge VARISPIN15R, Gyunggi-do, Korea). The supernatant was removed, and the pellet was resuspended in PBS to the OD_{600} of

approximately 0.5 that corresponds to ~3.4 × 10^8 CFU.mL^{-1}, from which a series of diluted suspension was prepared.

The optical density at 600 nm wavelength (OD_{600}) of the dilution series was measured using a microplate reader spectrophotometer (SpectraMax 190, Molecular Devices LLC, San Jose, CA, USA). The optical OD_{600} of the suspension was corrected for a blank PBS solution. A 20 µL of each dilution was plated on an LB agar for cell counting, and the OD_{600} of dilution series was correlated with the cell counting in CFU.mL^{-1}. Figure 3 illustrates the procedures for standard curve generation and cell counting.

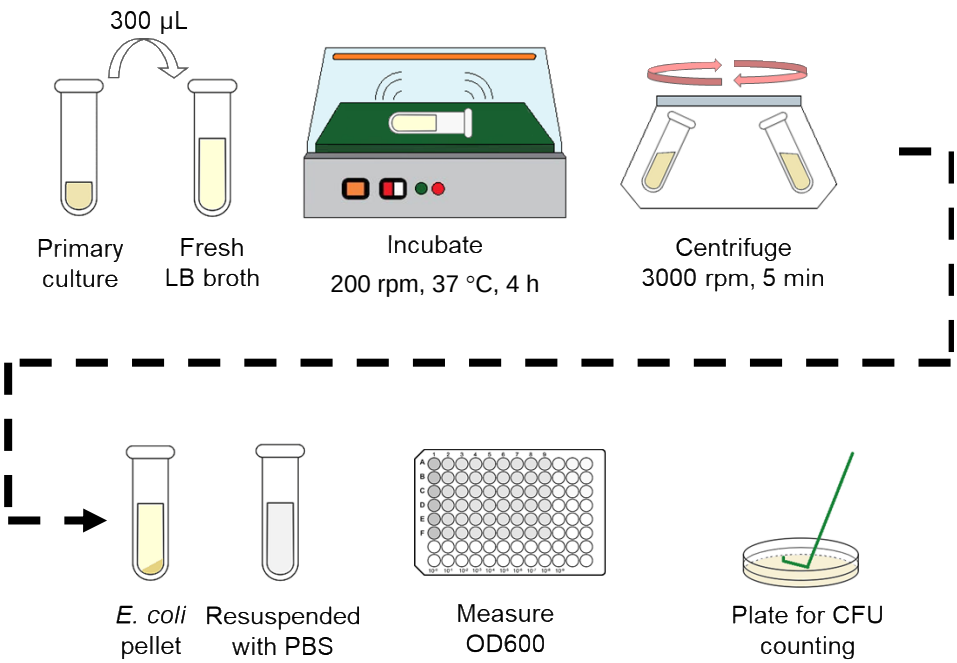

Figure 2. Method 1: Standard curve for optical density and cell counting. CFU = colony-forming unit.

Extraction of surface-adhered bacteria. For detachment of bacteria, the bacteria-adhered nonwoven substrate was placed in a centrifuge tube containing 0.5 mL of 0.1% sodium dodecyl sulfate (SDS)/PBS solution and 0.5 mL of TrypLE Express Enzyme; then the solution was sonicated in an ultrasonic bath for 5 min at 37 °C (60 Hz with the power output of 300 W). After sonication, tubes were shaken at 1400 rpm for 5 min at room temperature, using a micromixer (Thermo micromixer Mxi4t, FINEPCR, Gyeonggi-do, Korea).

Each sample was extracted three times, using a fresh solution with SDS surfactant and TrypLE Express Enzyme. Three extracts with detached bacteria cells were combined for measurement of OD_{600}. The number of CFU was correlated with the OD_{600} measurement and expressed as $CFU.mL^{-1}$ solution or $CFU.cm^{-3}$ substrate surface (**Figure 3**).

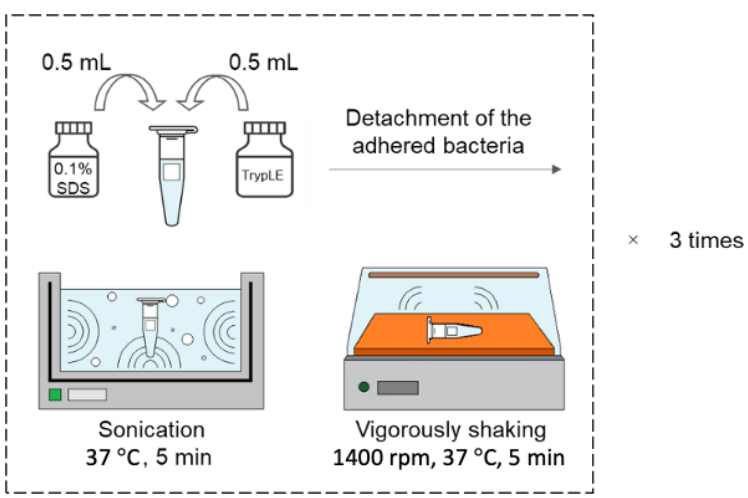

Figure 3. Method 1: Extraction of surface-adhered bacteria and cell counting.

4.2.2. Method 2: Colorimetric method

Standard curve for color absorbency and cell counting. One mL of bacteria suspension in PBS was transferred to a tube, 200 μL of 9.9×10^{-3} mol INT stock solution and 1 mL of PBS was added to the suspension, followed by incubation with 100 rpm for 4 h, at 37 °C. During incubation, the tetrazolium salt was reduced by accepting the electrons of active cells, and formazan was formed.

The formazan-formed culture suspension was pelleted at 14,000 rpm for 30 min. The colorless supernatant was then removed, and the pelleted formazan in red color was resuspended in 2 mL of DMSO by sonicating for 2 min to extract the formazan (colorant) to DMSO.

For a thorough transfer of formazan to DMSO, the suspension was heated up to around 105 °C for 5 min. The suspension solution was then filtered through a microfilter (0.22 μm pore), and dilution series of INT-DMSO eluent were prepared for absorbency measurement at the wavelength of 470 nm using a spectrophotometer. The procedure is illustrated in **Figure 4**.

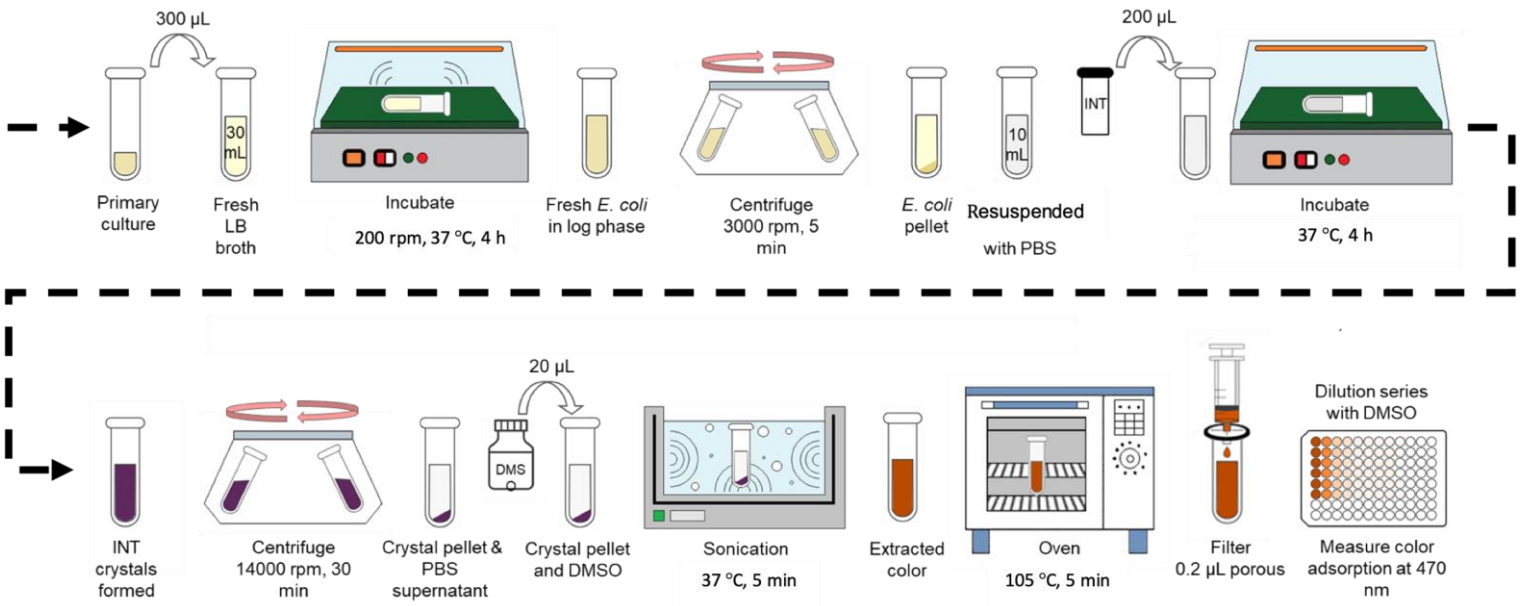

Figure 4. Method 2: Standard curve for color absorbency and cell counting.

Colorimetric measurement. To estimate the number of adhered bacteria that contributed to formazan formation, the bacteria-adhered substrates were incubated with 100 rpm for 4 h, at 37 °C, in a 24-well plate containing 200 µL of 9.9×10^{-3} mol INT stock solution and 1 mL of PBS. After incubation with INT, samples were moved to a new plate, and the formazan was extracted with DMSO; the suspension in DMSO was heated to about 105 °C for 5 min for complete extraction.

The suspension was then filtered through a microfilter (0.22 µm pore), and the INT formazan/DMSO eluent was measured for its absorbency at the wavelength of 470 nm using a spectrophotometer. The number of adhered bacteria was correlated with OD_{470} measurement and expressed as $CFU.mL^{-1}$ solution or $CFU.cm^{-3}$ substrate surface. Pictures of substrates after being stained by INT and after being extracted with DMSO were taken as proof of the complete extraction of INT formazans by DMSO (**Figure 5**).

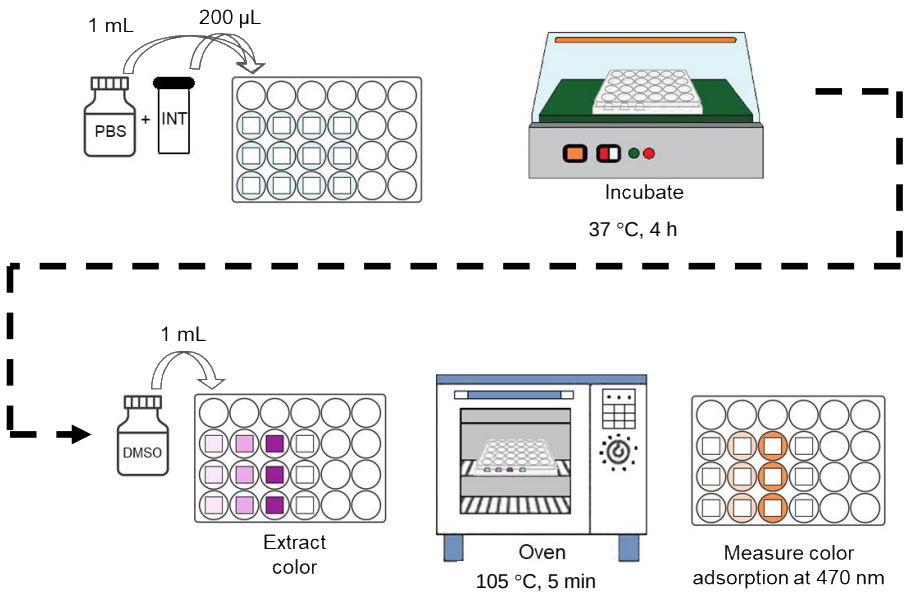

Figure 5. Method 2: Colorimetric analysis with INT staining of bacterial cells.

Chapter 3. Results and Discussion

3.1. Comparison of bacterial adhesion assay methods

Three different quantification methods were examined for measuring the number of adhered bacteria to film and nonwoven fibrous surfaces. In the extraction method, where the CFU was linearly correlated with OD_{600}, both live and dead cells were countable; however, complete detachment of bacteria could not be assured, especially for porous and depth-layered substrates.

For the colorimetric method, the bacteria detachment procedure is not necessary. Also, the INT reaction only affected the live bacterial cells, thus, the color signal did not interfere with the background noise from the polymer staining. Direct visualization of bacteria presence was possible with the naked eye by the INT staining (Figure 6). Disadvantage of the colorimetric method is the limited detection range; however, for CFU $\leq 5.9 \times 10^8$ a linear relationship between OD_{470} and CFU was obtained through the colorimetric method.

In the microscopic analysis, direct observation of bacterial distribution on surfaces was possible, yet the accurate quantification was very limited, especially for porous, multi-layered surfaces. Three different methods, their relevancy, and limitations in quantification of surface-adhered bacteria are summarized in Table 2.

To investigate whether the absorbency of formazan is in direct correlation with the number of live bacteria, a fitted line was generated by correlating the OD_{470} with CFU (**Figure 7**). When reacting with INT of 1.98×10^{-6} mol (200 μl of 9.9×10^{-3} mol), a linear increase of absorbency with the viable cell numbers was observed up to about 6.6×10^{8} CFU, and thereafter the OD_{470} reached a plateau. To examine whether the additional amount of INT affects the color absorbency over CFU~ 6.6×10^{8}, INT amount was doubled (3.96×10^{-6} mol) to react with bacteria suspensions of 8.3×10^{8} CFU.mL^{-1} (OD_{600} ~ 1.2), 9.7×10^{8} CFU.mL^{-1} (OD_{600} ~ 1.4) and 11×10^{8} CFU.mL^{-1} (OD_{600} ~ 1.6), respectively.

From **Figure 7**, the OD_{470} with two different INT amounts overlapped for the tested suspensions, showing that 1.98×10^{-6} mol of INT were sufficient to react with bacteria cells. However, the linearity between OD_{470} and CFU was not met above the CFU~ 5.9×10^{8}, thus, the maximum detection limit of this method was determined to be 5.9×10^{8} cells.

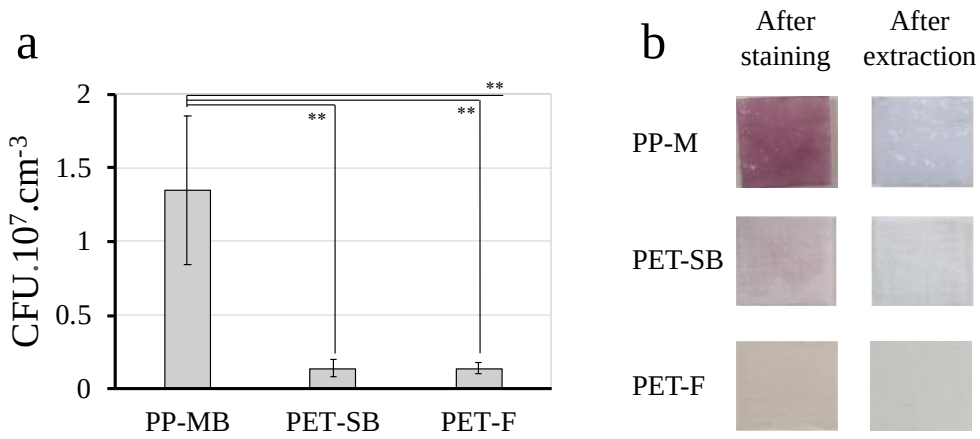

Figure 6. Measurement of substrate-adhered bacteria. (a) Quantification of CFU for different substrates; (b) Visual observation of formazan (reduced INT) crystals formed on substrates. Error bars represent the standard deviation of three individual nonwoven samples. (** $p < 0.01$).

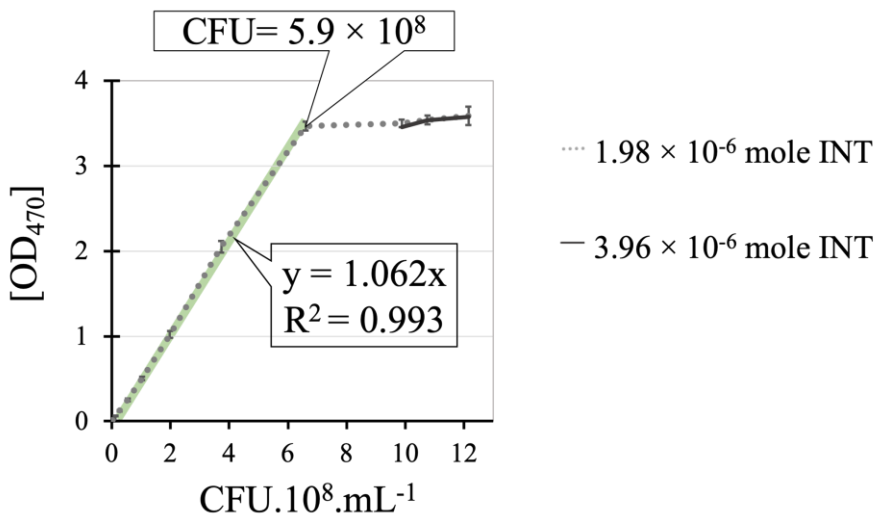

Figure 7. Relationship of OD_{470} and CFU for different INT concentrations.

Table 2. Comparison of bacterial adhesion assay methods.

Method	Relevancy	Limitation
Extraction	• Optical density of cell suspension linearly predicts the CFU. • Count both live and dead bacteria.	• Complete detachment of bacteria is not assured, especially for porous substrates.
Colorimetric	• bacteria detachment procedure is not necessary. • Visualization of bacterial presence is possible, even in the naked eye. • Count only the live cells.	• Detection limit exists. • Observation by the naked eye is difficult at the low level of bacterial concentration.
Microscopy	• Direct observation of bacterial distribution on surfaces is possible. • Only the topmost surface is observable.	• Quantification is not accurate. • Observation in-depth layer is not possible.

3.2. Effect of wettability on bacterial adhesion

Figure 8 shows the surface energy components and wettability of substrates. After plasma treatment, there was no considerable roughness observed either for O_2 plasma treated or C_4F_8 treated film surfaces. Therefore, it was assumed that plasma treatment only affected the surface energy, not the topography. The surface energy was estimated through employing the Owens-Wendt model by inputting the measured contact angles of surfaces [75]. The Owens-Wendt model assumes that the surface is smooth; thus, the surface energy value was calculated from the smooth film surfaces, then the surface energy of fibrous surface was regarded as the same. Practically, the prepared bacteria plateau may have some levels of surface roughness, but since we assumed it to be flat, the measured CAs in this study could be exaggerated.

In addition to the surface energy, the presence of surface roughness of fibrous substrates contributes to the wettability, as the Wenzel model [76] and Cassie-Baxter model [77] explain. Particularly, the Cassie-Baxter model [77] explains that the contact angle increases as the solid area fraction, which is in direct contact with the liquid drop, is reduced. From a rough surface where the air is trapped between the surface protrusions, the solid area fraction is less than 1, and this solid area fraction value determines the apparent contact angle, according

to the Cassie–Baxter model.

On the other hand, the Wenzel model [76] assumes that the droplet fully fills the cavity between the roughened protrusions, and the presence of surface roughness affects the apparent contact angle. Regardless of different assumptions, both theories commonly conclude that the existence of roughness intensifies the tendency of wettability of smooth surfaces. That is, when a smooth surface is hydrophobic with contact angle (CA) > 90, the roughened surface with the same surface energy further enhances the hydrophobicity; likewise, when roughness is introduced to a hydrophilic surface, it further increases the hydrophilic tendency on the rough surface [77].

The results of contact angles and surface energy components of all samples are shown in **Figure 8**. As reflected in **Figure 8,** the untreated PLA film and PS film showed different CAs 80, 103° and different surface energies 24.8–46.77 mN/m, due to the difference in their chemistry, a slight difference in both films' dispersive and polar components was observed. When the surfaces of PLA and PS were treated by C_4F_8 PECVD, the surface energy of both surfaces became very similar, 14.2–15.72 mN/m to the same level of polar and dispersive components as the same coating was applied.

The fluorinated surface showed higher CAs either for the films or the fibers compared to the untreated surfaces (**Figure 8a**). Likewise, O_2 plasma increased the substrate's polar components and the total

surface energy at a similar level, 51.57–53 mN/m for PLA and PS, enhancing the wettability. With hydrophilic surface modification, the CAs of O_2-treated substrates were decreased compared to the untreated substrates (**Figure 8a**).

The results for C_4F_8 and O_2 plasma treatments confirmed the successful modification of surface wettability, changing the surface energy components. Both bacteria showed low contact angles, 15–16° (**Figure 8a**). The results of the surface energies calculated from the contact angles are shown in **Figure 8b**, which demonstrates that both bacteria are hydrophilic, which is in accordance with Hamadi *et al.*'s study [78].

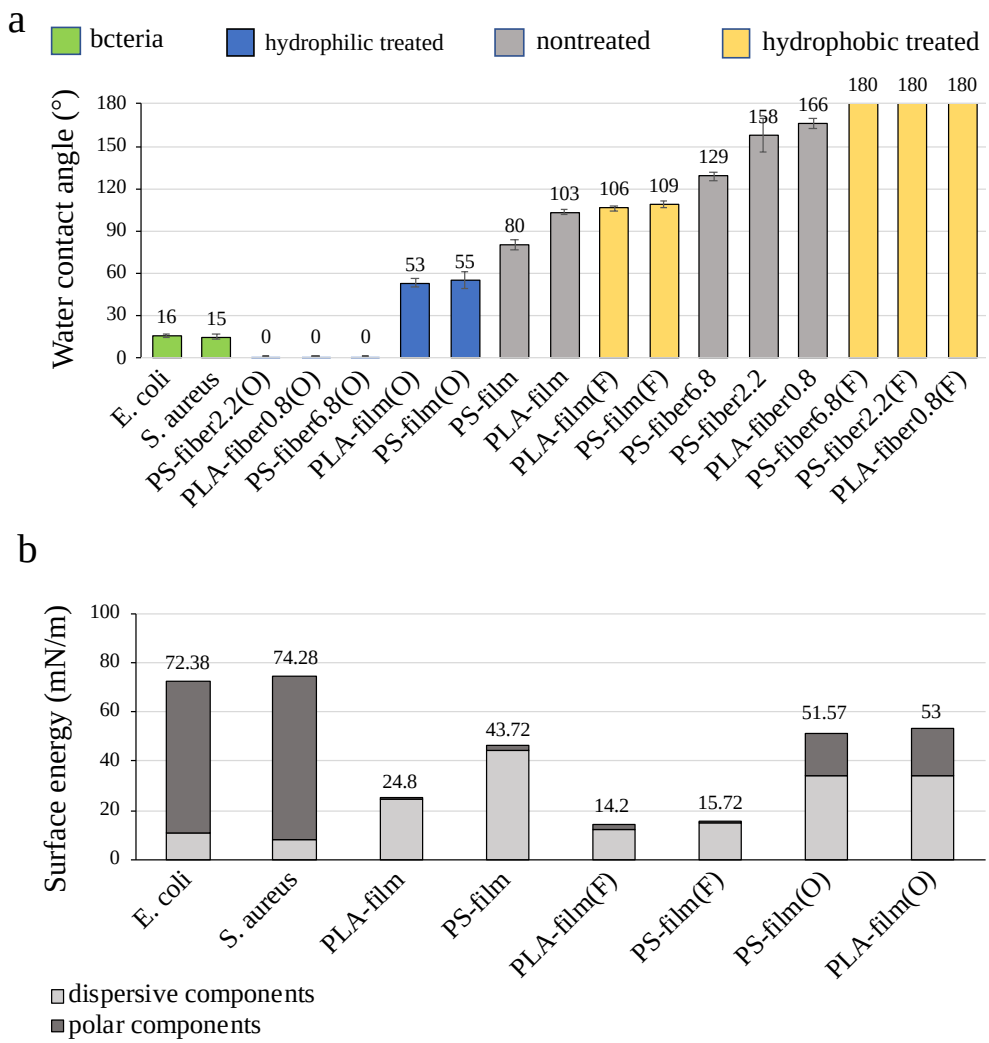

Figure 8. Surface energy and wettability. (a) Water contact angle of different surfaces; (b) Surface energy with polar and dispersive components of substates.

Accordingly, hydrophilic fiber samples with O_2 plasma-treated had higher bacterial adhesion compared to the hydrophobic substrates (Figure 9). The adhesion result was correlated with the wetting properties of substrate surfaces. The bacteria tested in this research

were evaluated to be hydrophilic and demonstrated favorable attachment to the hydrophilic substrates [44,45]. During PBS rinsing process, the bacteria attached to the hydrophobic surfaces were easily detached because of weak interaction with the surfaces. From the results, the wettability of the substrates was a dominant factor affecting the bacterial adhesion, in which hydrophilic surfaces showed higher adhesion.

As shown in **Figure 10**, the bacterial adhesion for both *E. coli* and *S. aureus* decreased as the substrates' CA increased. However, the result was at odds with previous research [46–48], in which *E. coli* with a lipopolysaccharide cell wall was likely to attach better on the hydrophobic surfaces. According to previous studies, wetting characteristics of bacteria are significantly regulated by environmental conditions. Hence, it is still controversial whether *E. coli* would show favorable adherence on hydrophilic or hydrophobic surfaces since many factors are involved [49–51]. As the bacteria and the substrates were incubated in aqueous media, the hydrophilic medium would favor interacting with the hydrophilic substrates, effectively carrying the cells into the fibrous substrates. A similar result was reported by Bajpai *et al.* [31], in which hydrophobic fabrics including polyester, did not show much *E. coli* adhesion.

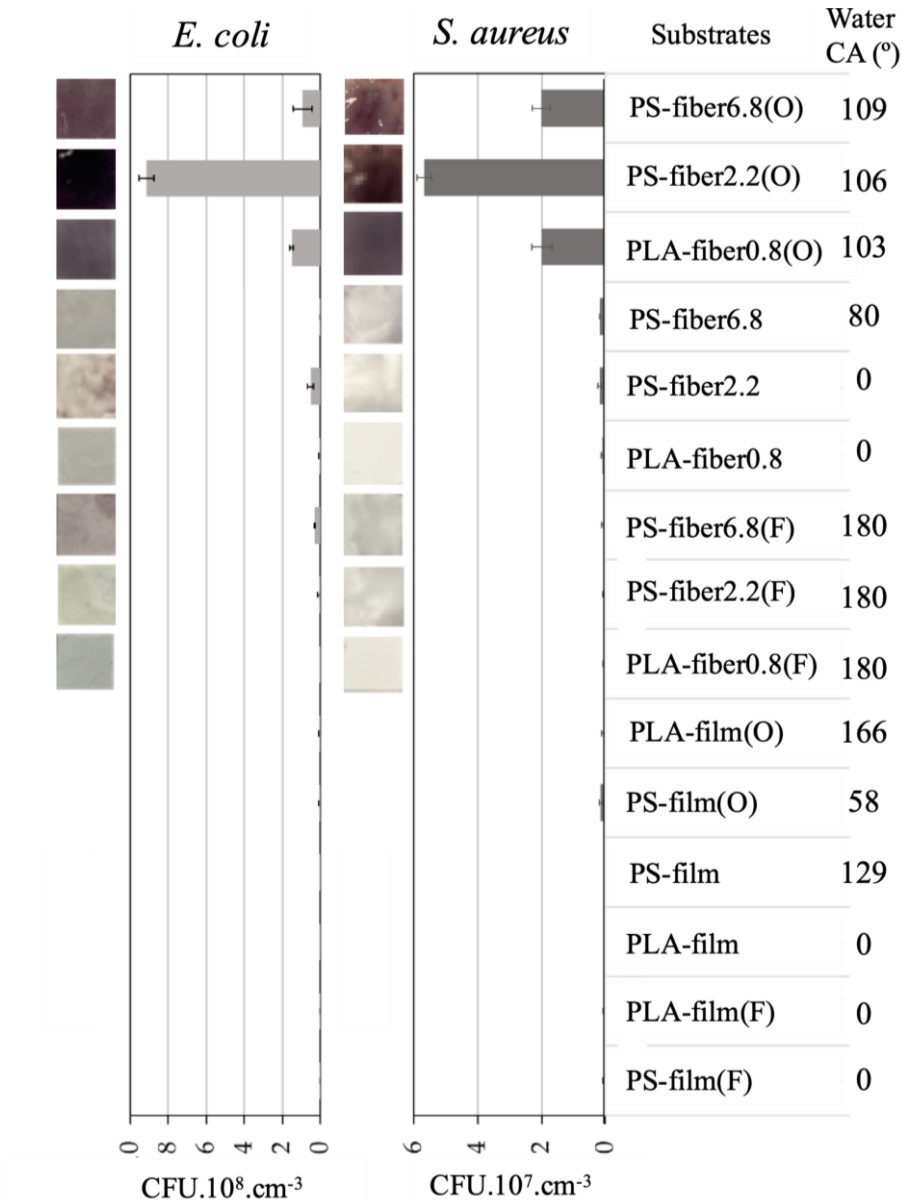

Figure 9. Bacterial adhesion on varied substrates. INT staining of *E. coli* and *S. aureus* adhered on substrates. Higher intensity of purple color represents higher bacterial adhesion on fabric substrates.

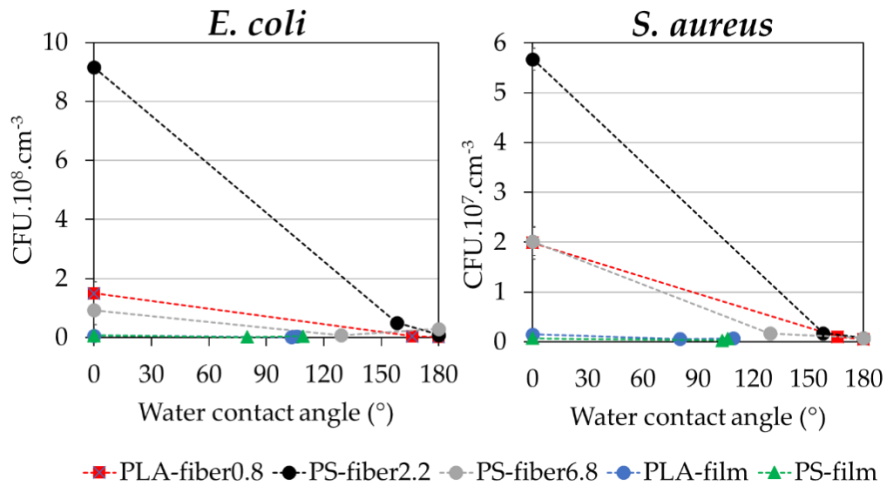

Figure 10. *E. coli* and *S. aureus* adhesion rate as a function of surface contact angle.

The wettability alone cannot explain the significant difference of adhesion between hydrophilic films and hydrophilic fibers (Figure 10). Thus, the wettability may not be the only factor affecting the adhesion, but other factors such as pore structure or porosity of fibers may also participate in bacterial adhesion. Even though nonwovens' the most distinctive characteristic that might affect bacterial adhesion is porosity, there have been few studies that explain the effect of pore characteristics on bacterial adhesion as well. This study is novel in that it paticularly discusses varied morphological characteristics of nonwovens including, porosity percentage, total pore volume, and pore size distribution in association with bacterial adhesion.

SEM images of *E. coli* and *S. aureus* strains adhered on different fibers are shown in Figure 11. Both *E. coli* and *S. aureus* had a similar

adhesion trend, but with a higher adherence for *E. coli.* The rod-shaped *E. coli* would have a larger interactive surface area than the *S. aureus* with a spherical shape, which may have affected the number of adhered cells [52–54].

In general, O_2 plasma-treated hydrophilic substrates showed a high bacterial adhesion, while C_4F_8-treated, superhydrophobic substrates showed a very low bacterial adhesion. However, unlike the quantitative measurements shown in **Figure 10,** SEM images (**Figure 11)** only provide qualitative information observation of surface adherence. It does not display the cells adhered inside the pores of the substrate; thus, the observed adhesion may not accurately represent the total number of adhered bacteria. Effects of pore characteristics including total pore volume and pore size on the adhesion were further investigated.

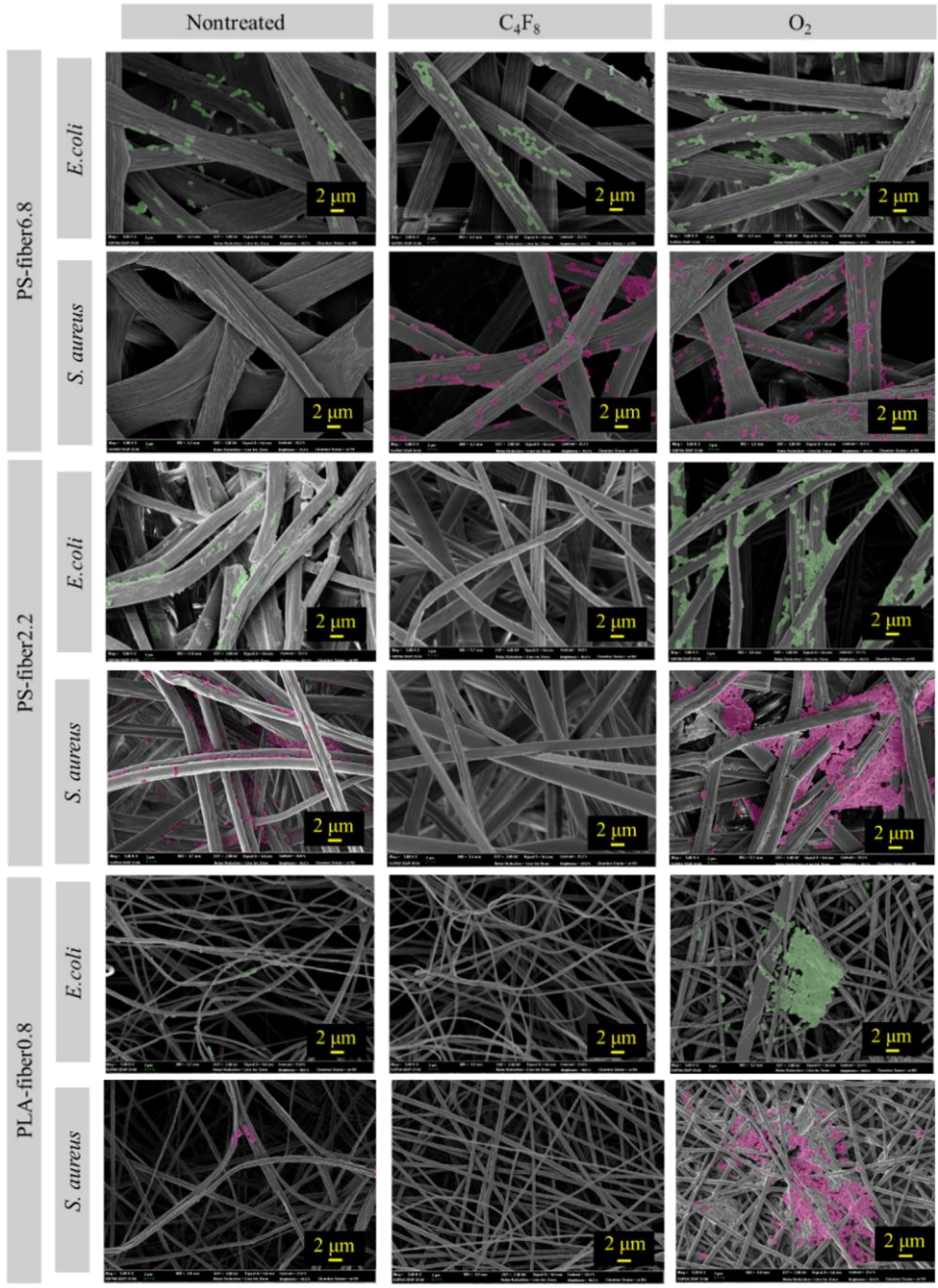

Figure 11. *E. coli* and *S. aureus* adhesion on different substrates. Adhered *E. coli* and *S. aureus* on fibers are marked with green and pink color, respectively.

3.3. Effect of Nonwoven substrate's morphology and pore characteristics on bacterial adhesion

From **Figure 11,** the tendency of cell adhesion on different substrates was observed. Bacteria were rarely observed in film surfaces; thus, the images of films were not included. For PS-fiber6.8 with a larger fiber diameter, most bacteria were observed on the fiber surface, and little was observed in the space between the fibers. For PS-fiber2.2, relatively high amount of cells was observed on inner surfaces between the fibers.

PLA-fiber0.8 webs with the smallest fibers were densely packed rather than other fibrous webs. A higher loading of bacteria on the surface was observed for PLA-fiber0.8, where the surface pores of the web were clogged by the cells. Compactness of fibers seemed to limit bacterial cells' depth loading, somewhat limiting the intrusion of bacteria into the inner pores.

While the extent of surface-adhered bacteria looked similar for PLA-fiber0.8 and PS-fiber2.2, the quantitative measurement of cells from the extracts revealed a higher cell loading for PS-fiber2.2 (**Figure 9**). It can be speculated that more bacterial cells were present inside the pores of the web for PS-fiber2.2 than for PLA-fiber0.8, resulting in higher total adhesion in the volume. Assuming that the total pore volume and/or pore size of substrates would affect the cell adhesion, the pore characteristics were further investigated.

In **Figure 12**, the solidity of the fibrous substrate is illustrated. The solidity of films was estimated to be 1 considering zero inner pores in films (porosity 0%). Compared to the film substrate, fibrous web had a considerably small solidity value with a notable value for porosity [55]. The film, which had a smooth surface with zero porosity, showed a lower level of bacterial adhesion compared to electrospun webs, regardless of surface treatments. It appeared that a smooth surface with little to zero porosity is advantageous for the antifouling property, as the bacterial cells cannot intrude into the pores for a firm attachment. Particularly, the surface with little surface roughness and no pores makes bacterial adhesion unstable, leading to easy detachment when applying the mechanical stress throughout rinsing process.

On the contrary, fiber webs with random surface roughness and high porosity showed much higher bacterial adhesion (**Figure 12b** and **Figure 12c**) [31,32,34]. Similar to the preceding, Bajpai *et al.* [14] demonstrated that fabrics with a rough surface, such as cotton, had a high bacterial adherence. Roughness grooves and random-sized pores that are accessible from the web surface would allow strong attachment of bacteria. Once bacteria settle inside the pore, they are hardly detached with the external stress due to rinsing.

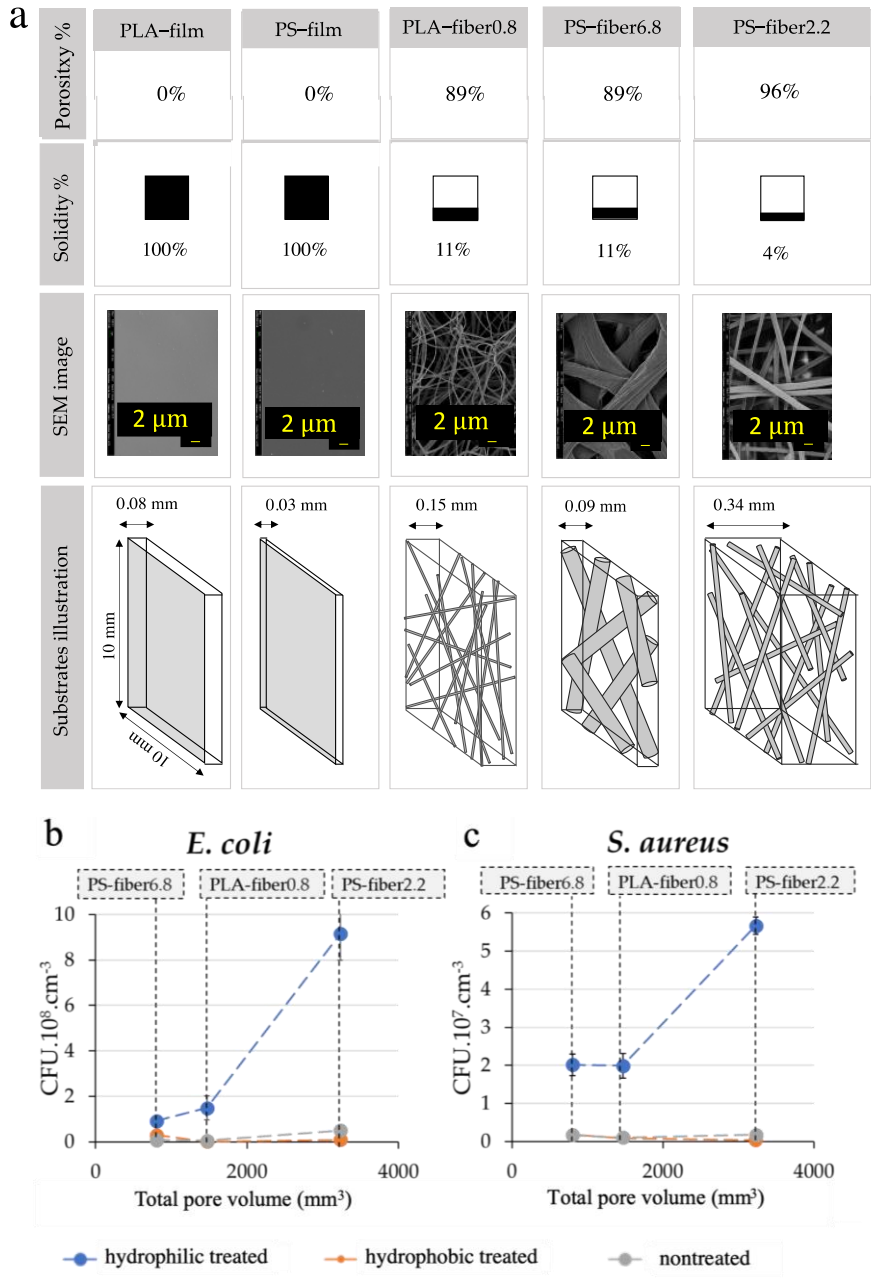

Figure 12. Morphology and pore characteristics of substrates. (a) Porosity, solidity, SEM image and schematic illustration of the relative size of fibers and pores for different substrates; (b) *E. coli* adhesion with a varied total pore volume of substrates; (c) *S. aureus* adhesion with a varied total pore volume of substrates.

Among the O_2-treated hydrophilic substrates, PS-fiber2.2(O) with the largest porosity (96%) showed the highest adhesion rate. Porosity percentage seems to play an important role in bacterial adhesion. According to **Figure 12a**, both PLA-fiber0.8(O) and PS-fiber6.8(O) has the same porosity and also similar low adhesion rate compared to PS-fiber2.2(O) (**Figure 9**). Based on the results, total pore volume, rather than fiber diameter, appeared to be an important factor influencing the bacterial adhesion. In this study, the apparent volume and the total pore volume were calculated by equations (3) and (4), and the total pore volume was analyzed as an important factor affecting the bacterial adhesion. The porosity percentage, apparent substrate volume, and the web's total pore volume are related.

According to **Table 1**, PS-fiber2.2 had the highest apparent volume (34 mm^3) and highest porosity (96%), with a much fluffier structure and the highest total pore volume (3230 mm^3). A large volume of total pores with hydrophilic nature allowed significantly higher bacterial adhesion, where the inner pores acted as trap sites for bacteria that penetrated into the substrates. Once bacteria were trapped inside the sample, it was difficult to detach the cells from the web. **Figure 12** demonstrates that the higher total pore volume of PS-fiber2.2(O) affected the higher amount of adhered bacteria on the web. Compared to PS-fiber2.2(O), almost same amount of bacteria were adhered on PLA-fiber0.8(O) and PS-fiber6.8(O), which had the same porosity

(89%) but different total pore volumes of 1470 mm^3 and 801 mm^3, respectively. For PS-fiber6.8(O) with large sized pores, it is speculated that bacteria easily intrude but they are also easily detached from the nonwoven substrates. For PLA-fiber0.8(O) with the smallest pore size, penetration of bacteria into the web seemed to be limited because of the compact structure of the substrate, resulting in lower adhesion rate.

Karger *et al.* [56] demonstrated that bacteria preferred to adhere to the gap between the fibers, and our finding corresponded to this result. In this study, PS-fiber6.8 with the lowest thickness (0.09 mm) revealed to have the smallest total pore volume (801 mm^3). From the results, bacterial adhesion was indeed affected by the fiber morphology and pore characteristics of nonwoven substrates. The effect of pore characteristics on the bacterial adhesion was further examined in terms of pore size distributions of PS-fiber2.2, PS-fiber6.8, and PLA-fiber0.8 (**Figure 13**).

PLA-fiber0.8 showed a narrower size distribution (1~3 μm) with smaller pores, while PS-fiber6.8 depicted a wider size distribution with larger pores (3~26 μm). Although PLA-fiber0.8 and PS-fiber6.8 had similar porosity (89%), they presented a considerable difference in pore size distribution. While the total pore volume itself seemed to be an influential factor for the bacterial adhesion, the relative size of pores to the cell was another factor determining the bacrerial adhesion

and retention. When the pore size is too large, bacteria would easily intrude in the web pores, but they would also easily escape. If the pore size is too small or not large enough to endure bacteria, bacteria cannot properly intrude the pores but bump into the surface, leading to the easy isolation from the substrates.

For such reasons, the PS-fiber2.2(O), which showed pores of 2—12 μm with a high total pore volume, showed a higher bacterial adhesion than the substrates with similar wettability. PS-fiber6.8 had much larger pores of 3-26 μm, which would allow easier de-trapping of adhered bacteria. From the SEM images of PS-fiber6.8 in **Figure 11**, bacteria adhered to the fiber surface, but they were rarely observed between the fibers; the bacteria observed on the fiber surface can be detached rather easily during the rinsing process.

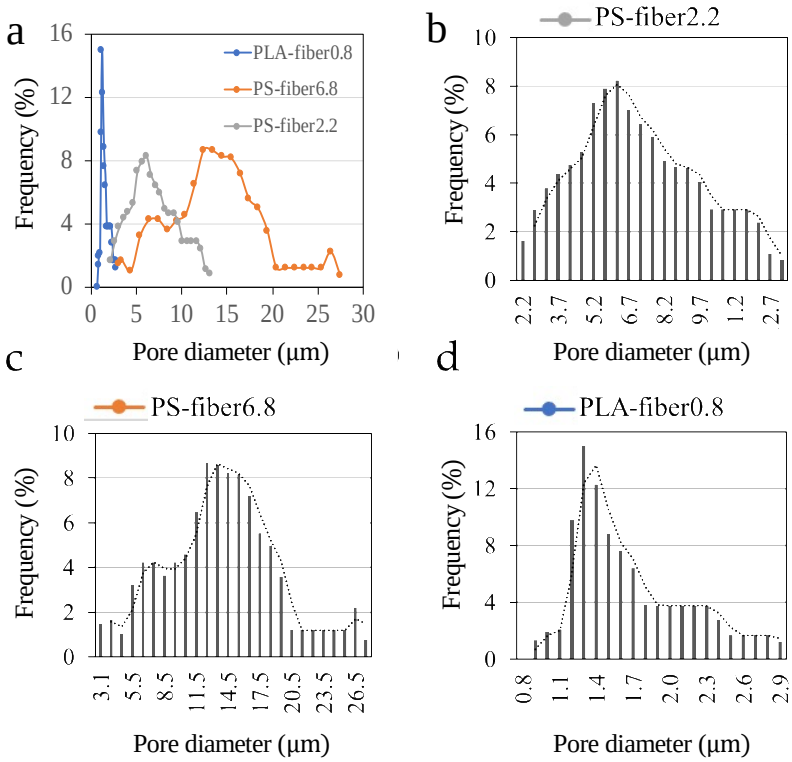

Figure 13. Pore size distribution of substrates. (a) All electrospun webs; (b) PS-fiber2.2; (c) PS-fiber6.8; (d) PLA-fiber0.8.

With the growing concerns about the spreading of infectious diseases by bacteria, it is imperative to control the bacterial adhesion and its growth on nonwoven substrates. This study is concerned with identifying textile parameters and design insights contributing to the control of bacterial adhesion in liquid medium. Textiles as porous substrates, the pore volume, and the pore size distribution of the substrate need to be included as important design parameters. The results indicated that wettability, pore size, and total pore volume were involved with bacterial adhision and retention on the substrate.

The results of this study can be applicable for designing disposable hygiene textiles or protective equipment made of nonwovens. For example, a superhydrophobic nonwoven web with the compacat structure and small pore size (pore size 0.5-2 μm) would be advantageous in circumventing the adhesion, and may be applied to protective clothing. A superhydrophobic web with large pore size and lower porosity (%) may be relevant for hygine application where adhered bacteria can be easily removed by washing procedure. It is still challenging to predict the adhesion with the factor of time. Further research is needed on the long-term biofouling, such as biofilm formation, to disclose the ambiguity of the adhesion mechanism as a function of time.

Chapter 4. Summary and Conclusions

In the first part of this study, a bacterial adhesion assay method was validated for its relevancy of application to nonwoven substrates-adhered bacteria by comparing three different methods for quantifying the adhered bacteria to polymeric substrates. For the substrates with pores and multi-layered fibers, the colorimetric analysis with INT staining provided reliable and reproducible results. The formazan produced by the reaction of INT and bacteria was effectively separated by solvent extraction, and the amount of bacteria could be visually observed by the absorbency of the colorant.

In the second phase of the study, effect of nonwoven substrates parameters on bacterial adhesion in the liquid medium was investigated. Nonwoven substrates parameters investigated were wettability, surface energy, porosity percentage, pore-volume, pore size distributions, and fiber diameter. Surface wettability showed to be an important factor influencing bacterial adhesion. The substrate's surface chemistry with its polar and disperse components of surface energy appeared the bacterial adhesion. The hydrophilic bacteria strains tested in this study tend to adhere to hydrophilic substrates more than hydrophobic substrates. Fibrous morphology not only affected the wettability but also provided a large surface area for bacterial adhesion. Total pore volume and pore size, rather than the

porosity % itself were important factors affecting the bacterial adhesion and retention. Low total pore volume with large pores prevented bacteria from being trapped inside the pores, leading to the reduced bacterial retention in the substrate.

The result of this study is significant in that pore characteristics, which are unique factors for the nonwoven substrate, were considered in interpreting the interaction between bacterial cells and fibrous substrates. By understanding the substrate parameters affecting the bacterial adhesion, textile design for circumventing the bacterial adhesion could be suggested. Findings of this study would contribute to developing anti-biofouling textiles with potential applications to hygiene products and protective garments against microbial infections.

Chapter 5. References

1. Lorenzetti, M.; Dogša, I.; Stošicki, T.; Stopar, D.; Kalin, M.; Kobe, S.; Novak, S. The Influence of surface modification on bacterial adhesion to titanium-based substrates. *ACS Appl. Mater. Interfaces.* 2015 Jan 28;7(3):1644-51.

2. Damodaran, V.B.; Murthy, N.S. Bio-inspired strategies for designing antifouling biomaterials. *Biomaterials*. 2016 Dec 20;(1):1-11.

3. Hori, K.; Matsumoto, S. Bacterial adhesion: from mechanism to control. *Biochem. Eng. J.I.* 2010 Feb 15;48(3):424-34.

4. Dhand, C.; Harini, S.; Venkatesh, M.; Dwivedi, N.; Ng, A.; Liu, S.; Verma, N.K.; Ramakrishna, S.; Beuerman, R.W.; Loh, X.J., Lakshminarayanan, R. Multifunctional polyphenols-and catecholamines-based self-defensive films for health care applications. *ACS Appl. Mater. Interfaces*. 2016 Jan 20;8(2):1220-32.

5. Wang, B.; Jin, T.; Xu, Q.; Liu, H.; Ye, Z.; Chen, H. Direct loading and tunable release of antibiotics from polyelectrolyte multilayers to reduce bacterial adhesion and biofilm formation. *Bioconjugate Chem.* 2016 May 18;27(5):1305-13.

6. Ong, Y.L.; Razatos, A.; Georgiou, G.; Sharma, M.M. Adhesion forces between E. coli bacteria and biomaterial surfaces. *Langmuir.* 1999 Apr 13;15(8):2719-25.

7. Galante, A.J.; Haghanifar, S.; Romanowski, E.G.; Shanks, R.M.; Leu, P.W. Superhemophobic and antivirofouling coating for mechanically durable and wash-stable medical textiles. *ACS Appl. Mater. Interfaces*. 2020 Apr 22;12(19):22120-8.

8. Nguyen, D.H.; Pham, V.T.; Truong, V.K.; Sbarski, I.; Wang, J.; Balčytis, A.; Juodkazis, S.; Mainwaring, D.E.; Crawford, R.J.; Ivanova, E.P. Role of topological scale in the differential fouling of Pseudomonas aeruginosa and Staphylococcus aureus bacterial cells on wrinkled gold-coated polystyrene surfaces. *Nanoscale*. 2018 Feb 7;10(11):5089-96.

9. Truong, V.K.; Lapovok, R.; Estrin, Y.S.; Rundell, S.; Wang, J.Y.; Fluke, C.J.; Crawford, R.J.; Ivanova, E.P. The influence of nano-scale surface roughness on bacterial adhesion to ultrafine-grained titanium. *Biomaterials*. 2010 May 1;31(13):3674-83.

10. Landry, K.S.; Morey, J.M.; Bharat, B.; Haney, N.M.; Panesar, S.S. Biofilms—impacts on human health and its relevance to space travel.

Microorganisms. 2020 Jul 3;8(7):998.

11. Eid, B.M.; Ibrahim, N.A. Recent developments in sustainable finishing of cellulosic textiles employing biotechnology. *J. Clean. Prod.* 2020 Oct 17;124701.

12. Karim, N.; Afroj, S.; Lloyd, K.; Oaten, L.C.; Andreeva, D.V.; Carr, C.; Farmery, A.D.; Kim, I.D.; Novoselov, K.S. Sustainable personal protective clothing for healthcare applications: a review. *ACS Nano.* 2020 Aug 31;14(10):12313-40.

13. Abd Elgadir, M.; Uddin, M.S.; Ferdosh, S.; Adam, A.; Chowdhury, A.J.; Sarker, M.Z. Impact of chitosan composites and chitosan nanoparticle composites on various drug delivery systems: a review. *J. Food Drug Anal.* 2015 Dec 1;23(4):619-29.

14. Gokce, Y.; Aktas, Z.; Capar, G.; Kutlu, E.; Anis, P. Improved antibacterial property of cotton fabrics coated with waste sericin/silver nanocomposite. *Mater. Chem. Phys.* 2020 Nov 1;254:123508.

15. Zhang, S.; Wang, L.; Liang, X.; Vorstius, J.; Keatch, R.; Corner, G.; Nabi, G.; Davidson, F.; Gadd, G.M.; Zhao, Q. Enhanced antibacterial and antiadhesive activities of silver-PTFE nanocomposite coating for urinary catheters. *ACS Biomater. Sci. Eng.* 2019 May 2;5(6):2804-14.

16. Gadkari, R.R.; Ali, S.W.; Joshi, M.; Rajendran, S.; Das, A.; Alagirusamy, R. Leveraging antibacterial efficacy of silver loaded chitosan nanoparticles on layer-by-layer self-assembled coated cotton fabric. *Int. J. Biol. Macromol.* 2020 Nov 1;162:548-60.

17. Swar, S.; Máková, V.; Horáková, J.; Kejzlar, P.; Parma, P.; Stibor, I. A comparative study between chemically modified and copper nanoparticle immobilized Nylon 6 films to explore their efficiency in fighting against two types of pathogenic bacteria. *Eur. Polym. J.* 2020 Jan 5;122:109392.

18. Prorokova, N.P.; Kumeeva, T.Y.; Agafonov, A.V.; Ivanov, V.K. Modification of polyester fabrics with nanosized titanium dioxide to impart photoactivity. *Inorg. Mater. Appl. Res.* 2017 Sep 4;8(5):696-703.

19. Chen, C.C.; Wang, C.C. Crosslinking of cotton cellulose with succinic acid in the presence of titanium dioxide nano-catalyst under UV irradiation. *J. Sol-Gel Sci. Techn.* 2006 Jul 15;40(1):31-8.

20. Prorokova, N.; Kumeeva, T.; Kholodkov, I. Formation of coatings based on titanium dioxide nanosolson polyester fibre materials. *Coatings*. 2020 Jan 19;10(1):82.

21. Hu, J.; Zhang, M.; He, Y.; Zhang, M.; Shen, R.; Zhang, Y.; Wang, M.; Wu,

G. Fabrication and potential applications of highly durable superhydrophobic polyethylene terephthalate Fabrics produced by in-situ zinc oxide (ZnO) nanowires deposition and polydimethylsiloxane (PDMS) Packaging. *Polymers*. 2020 Oct 13;12(10):2333.

22. Hatamie, A.; Khan, A.; Golabi, M.; Turner, A.P.F.; Beni, V.; Mak, W.C.; Sadollahkhani, A.; Alnoor, H.; Zargar, B.; Bano, S., et al. Zinc oxide nanostructure-modified textile and its application to biosensing, photocatalysis, and as antibacterial material. *Langmuir*. 2015 Oct 6;31(39):10913-21.

23. Paladini, F.; Pollini, M.; Sannino, A.; Ambrosio, L. Metal-based antibacterial substrates for biomedical applications. *Biomacromolecules*. 2015 Jul 13;16(7):1873-85.

24. Hong, H.R.; Kim, J.; Park, C.H. Facile Fabrication of Multifunctional Fabrics: use of copper and silver nanoparticles for antibacterial, superhydrophobic, conductive fabrics. *RSC Adv.* 2018 Dec 13;8(73):41782-94.

25. Jiang, H.; Manolache, S.; Wong, A.C.; Denes, F.S. Plasma-enhanced deposition of silver nanoparticles onto polymer and metal surfaces for the generation of antimicrobial characteristics. *J. Appl. Polym. Sci.* 2004 Aug 5;93(3):1411-22.

26. Zille, A.; Fernandes, M.M.; Francesko, A.; Tzanov, T.; Fernandes, M.; Oliveira, F.R.; Almeida, L.; Amorim, T.; Carneiro, N.; Esteves, M.F.; Souto A.P. Size and aging effects on antimicrobial efficiency of silver nanoparticles coated on polyamide fabrics activated by atmospheric DBD plasma. *ACS Appl. Mater. Interfaces.* 2015 Jul 1;7(25:13731-44.

27. Tripathi, D.K.; Tripathi, A.; Shweta; Singh, S.; Singh, Y.; Vishwakarma, K.; Yadav, G.; Sharma, S.; Singh, V.K.; Mishra, R.K., Upadhyay, R.G.; Dubey, N.K. Uptake, accumulation and toxicity of silver nanoparticle in autotrophic plants, and heterotrophic microbes: a concentric review. *Front. Microbiol.* 2017 Jan 26;8:7.

28. Tay, C.Y.; Cai, P.; Setyawati, M.I.; Fang, W.; Tan, L.P.; Hong, C.H.; Chen, X.; Leong, D.T. Nanoparticles strengthen intracellular tension and retard cellular migration. *Nano Lett.* 2014 Jan 8;14(1):83-8.

29. Setyawati, M.I.; Yuan, X.; Xie, J.; Leong, D.T. The influence of lysosomal stability of silver nanomaterials on their toxicity to human cells. *Biomaterials.* 2014 Aug 1;35(25):6707-15.

30. Tay, C.Y.; Fang, W.; Setyawati, M.I.; Chia, S.L.; Tan, K.S.; Hong, C.H.; Leong, D.T. Nano-hydroxyapatite and nano-titanium dioxide exhibit different subcellular distribution and apoptotic profile in human oral

epithelium. *ACS Appl. Mater. Interfaces*. 2014 May 14;6(9):6248-56.

31. Rivera Gil, P.; Oberdörster, G.; Elder, A.; Puntes, V.; Parak, W.J. Correlating physico-chemical with toxicological properties of nanoparticles: the Present and the Future. *ACS Nano.* 2010 Oct 26;4(10):5527-31.

32. Setyawati, M.I.; Tay, C.Y.; Chia, S.L.; Goh, S.L.; Fang, W.; Neo, M.J.; Chong, H.C.; Tan, S.M.; Loo, S.C.J.; Ng, K.W., et al. Titanium dioxide nanomaterials cause endothelial cell leakiness by disrupting the homophilic interaction of VE-cadherin. *Nat. Commun.* 2013 Apr 9;4(1):1-2.

33. Kohanski, M.A.; Dwyer, D.J.; Collins, J.J. How antibiotics kill bacteria: from targets to networks. *Nat. Rev. Microbiol.* 2010 May 4;8(6):423-35.

34. Eid, B.M.; El-Sayed, G.M.; Ibrahim, H.M.; Habib, N.H. Durable antibacterial functionality of cotton/polyester blended fabrics using antibiotic/MONPs composite. *Fiber. Polym.* 2019 Dec 2;20(11):2297-309.

35. Montagut, A.M.; Granados, A.; Lazurko, C.; El-Khoury, A.; Suuronen, E.J.; Alarcon, E.I.; Sebastián, R.M.; Vallribera, A. Triazine mediatedv covalent antibiotic grafting on cotton fabrics as a modular approach for developing antimicrobial barriers. *Cellulose.* 2019 Jul 5;26(12):7495-505.

36. Cheng, X.; Zhang, W.; Ji, Y.; Meng, J.; Guo, H.; Liu, J.; Wu, X.; Xu, H. Revealing silver cytotoxicity using Au nanorods/Ag shell nanostructures: disrupting cell membrane and causing apoptosis through oxidative damage. *RSC Adv.* 2013 Dec 4;3(7):2296-305.

37. Zeng, L.; Wu, Y.; Xu, J.-F.; Wang, S.; Zhang, X. Supramolecular switching surface for antifouling and bactericidal activities. *ACS Appl. Bio Mater.* 2019 Jan 24;2(2):638-43.

38. AshaRani, P.V.; Low Kah Mun, G.; Hande, M.P.; Valiyaveettil, S. Cytotoxicity and genotoxicity of silver nanoparticles in human cells. *ACS Nano.* 2009 Feb 24;3(2):279-90.

39. Fiedot-Toboła, M.; Ciesielska, M.; Maliszewska, I.; Rac-Rumijowska, O.; Suchorska-Woźniak, P.; Teterycz, H.; Bryjak, M. Deposition of zinc oxide on different polymer textiles and their antibacterial properties. Materials. 2018 Apr 30;11(5):707.

40. Karakurt, I.; Ozaltin, K.; Vesela, D.; Lehocky, M.; Humpolíček, P.; Mozetič, M. Antibacterial activity and cytotoxicity of immobilized

glucosamine/chondroitin sulfate on polylactic acid films. *Polymers.* 2019 Jul 15;11(7):1186.

41. Wang, J.; Huang, N.; Yang, P.; Leng, Y.X.; Sun, H.; Liu, Z.Y.; Chu, P.K. The effects of amorphous carbon films deposited on polyethylene terephthalate on bacterial adhesion. *Biomaterials.* 2004 Jul 1;25(16):3163-70.

42. Rochford, E.T.J.; Poulsson, A.H.C.; Varela, J.S.; Lezuo, P.; Richards, R.G.; Moriarty, T.F. Bacterial adhesion to orthopaedic implant materials and a novel oxygen plasma modified PEEK surface. *Colloids Surf. B.* 2014 Jan 1;113:213-22.

43. Triandafillu, K.; Balazs, D.J.; Aronsson, B.O.; Descouts, P.; Tu Quoc, P.; van Delden, C.; Mathieu, H.J.; Harms, H. Adhesion of Pseudomonas aeruginosa strains to untreated and oxygen-plasma treated poly (vinyl chloride) (PVC) from endotracheal intubation devices. *Biomaterials.* 2003 Apr 1;24(8):1507-18.

44. Feng, G.; Cheng, Y.; Wang, S.-Y.; Hsu, L.C.; Feliz, Y.; Borca-Tasciuc, D.A.; Worobo, R.W.; Moraru, C.I. Alumina surfaces with nanoscale topography reduce attachment and biofilm formation by Escherichia coli and Listeria spp. *Biofouling.* 2014 Nov 26;30(10):1253-68.

45. Bajpai, V.; Dey, A.; Ghosh, S.; Bajpai, S.; Jha, M.K. Quantification of bacterial adherence on different textile fabrics. *Int. Biodeter. Biodegr.* 2011 Dec 1;65(8):1169-74.

46. Alam, A.K.M.M.; Ewaldz, E.; Xiang, C.; Qu, W.; Bai, X. Tunable wettability of biodegradable multilayer sandwich-structured electrospun nanofibrous membranes. *Polymers.* 2020 Sep 15;12(9):2092.

47. De Cesare, F.; Di Mattia, E.; Zussman, E.; Macagnano, A. A study on the dependence of bacteria adhesion on the polymer nanofibre diameter. *Environ. Sci. Nano.* 2019 Mar 14;6(3):778-97.

48. Varshney, S.; Sain, A.; Gupta, D.; Sharma, S. Factors affecting bacterial adhesion on selected textile fibres. *Indian J. Microbiol.* 2020 Sep 1;61(1):31-7.

49. Schmidt-Emrich, S.; Stiefel, P.; Rupper, P.; Katzenmeier, H.; Amberg, C.; Maniura-Weber, K.; Ren, Q. Rapid assay to assess bacterial adhesion on textiles. *Materials.* 2016 Mar 30;9(4):249.

50. BinAhmed, S.; Hasane, A.; Wang, Z.; Mansurov, A.; Romero-Vargas Castrillón, S. Bacterial adhesion to ultrafiltration membranes: role of hydrophilicity, natural organic matter, and cell-surface macromolecules.

Environ. Sci. Technol. 2018 Jan 2;52(1):162–72.

51. Oh, J.K.; Yegin, Y.; Yang, F.; Zhang, M.; Li, J.; Huang, S.; Verkhoturov, S.V.; Schweikert, E.A.; Perez-Lewis, K.; Scholar, E.A., et al. The influence of surface chemistry on the kinetics and thermodynamics of bacterial adhesion. *Sci. Rep.* 2018 Nov 22;8(1):1–3.

52. Yuan, Y.; Hays, M.P.; Hardwidge, P.R.; Kim, J. Surface characteristics influencing bacterial adhesion to polymeric substrates. *RSC Adv.* 2017 Mar 3;7(23):14254–61.

53. Koubali, H.; El Louali, M.; Zahir, H.; Soufiani, S.; Mabrouki, M.; Latrache, H. Physicochemical characterization of glass and polyethylene surfaces treated with different surfactants and their effects on bacterial adhesion. *Int. J. Adhes. Adhes.* 2021 Oct 14;104:102754.

54. Maikranz, E.; Spengler, C.; Thewes, N.; Thewes, A.; Nolle, F.; Jung, P.; Bischoff, M.; Santen, L.; Jacobs, K. Different binding mechanisms of Staphylococcus aureus to hydrophobic and hydrophilic surfaces. *Nanoscale.* 2020 Sep 16;12(37):19267–75.

55. Salerno, M.B.; Logan, B.E.; Velegol, D. Importance of molecular details in predicting bacterial adhesion to hydrophobic surfaces. *Langmuir*. 2004 Nov 23;20(24):10625–9.

56. Evans-Hurrell, J.A.; Adler, J.; Denyer, S.; Rogers, T.G.; Williams, P. A Method for the enumeration of bacterial adhesion to epithelial cells using image analysis. *FEMS Microbiol. Lett.* 1993 Feb 1;107(1):77–82.

57. Caldwell, D.E.; Germida, J.J. Evaluation of Difference Imagery for Visualizing and Quantitating Microbial Growth. Can. *Can. J. Microbiol.* 1985 Jan 1;31(1):35–44.

58. An, Y.H.; Friedman, R.J. Laboratory methods for studies of bacterial adhesion. *J. Microbiol. Meth.* 1997 Aug 1;30(2):141–52.

59. Li, J.; Kleintschek, T.; Rieder, A.; Cheng, Y.; Baumbach, T.; Obst, U.; Schwartz, T.; Levkin, P.A. Hydrophobic liquid-infused porous polymer surfaces for antibacterial applications. *ACS Appl. Mater. Interfaces.* 2013 Jul 24;5(14):6704–11.

60. Asadishad, B.; Ghoshal, S.; Tufenkji, N. Method for the direct observation and quantification of survival of bacteria attached to negatively or positively charged surfaces in an aqueous medium. *Environ. Sci. Technol.* 2011 Oct 1;45(19):8345–51.

61. Stiefel, P.; Schneider, J.; Amberg, C.; Maniura-Weber, K.; Ren, Q. A Simple and rapid method for optical visualization and quantification of bacteria on textiles. *Sci Rep.* 2016 Dec 22;6(1):1–9.

62. Stiefel, P.; Schmidt-Emrich, S.; Maniura-Weber, K.; Ren, Q. Critical aspects of using bacterial cell viability assays with the fluorophores SYTO9 and propidium iodide. *BMC Microbiol.* 2015 Feb 18;15(1):1-9.

63. Disney, M.D.; Zheng, J.; Swager, T.M.; Seeberger, P.H. Detection of bacteria with carbohydrate-functionalized fluorescent polymers. *J. Am. Chem. Soc.* 2004 Oct 20;126(41):13343-6.

64. Link, A.J.; Tirrell, D.A. Cell surface labeling of Escherichia coli via copper(I)-catalyzed [3+ 2] cycloaddition. *J. Am. Chem. Soc.* 2003 Sep 17;125(37):11164-5.

65. Din, N.; Gilkes, N.R.; Tekant, B.; Miller, R.C.; Warren, R.A.J.; Kilburn, D.G. Non-hydrolytic disruption of cellulose fibres by the binding domain of a bacterial cellulase. *Nat Biotechnol.* 1991 Nov 1;9(11):1096-9.

66. Lin, J.; Chen, X.; Chen, C.; Hu, J.; Zhou, C.; Cai, X.; Wang, W.; Zheng, C.; Zhang, P.; Cheng, J., et al. Durably antibacterial and bacterially antiadhesive cotton fabrics coated by cationic fluorinated polymers. *ACS Appl. Mater. Interfaces.* 2018 Feb 21;10(7):6124-36.

67. Nakanishi, J.; Kikuchi, Y.; Takarada, T.; Nakayama, H.; Yamaguchi, K.; Maeda, M. Photoactivation of a substrate for cell adhesion under standard fluorescence microscopes. *J. Am. Chem. Soc.* 2004 Dec 22;126(50):16314-5.

68. Yu, Q.; Cho, J.; Shivapooja, P.; Ista, L.K.; López, G.P. Nanopatterned smart polymer surfaces for controlled attachment, killing, and release of bacteria. *ACS Appl. Mater. Interfaces.* 2013 Oct 9;5(19):9295-304.

69. Prévost, V.; Anselme, K.; Gallet, O.; Hindié, M.; Petithory, T.; Valentin, J.; Veuillet, M.; Ploux, L. Real-time imaging of bacteria/osteoblast dynamic coculture on bone implant material in an in vitro postoperative contamination model. *ACS Biomater. Sci. Eng.* 2019 May 22;5(7):3260-9.

70. Keller, N.; Bruchmann, J.; Sollich, T.; Richter, C.; Thelen, R.; Kotz, F.; Schwartz, T.; Helmer, D.; Rapp, B.E. Study of biofilm growth on slippery liquid-infused porous surfaces made from fluoropor. *ACS Appl. Mater. Interfaces.* 2019 Jan 15;11(4):4480-7.

71. Taylor, J.P.; Wilson, B.; Mills, M.S.; Burns, R.G. Comparison of microbial numbers and enzymatic activities in surface soils and subsoils using various techniques. *Soil Biol. Biochem.* 2002 Mar 1;34(3):387-401.

72. Böckelmann, U.; Szewzyk, U.; Grohmann, E. A new enzymatic method for the detachment of particle associated soil bacteria. *J. Microbiol. Meth.* 2003 Oct 1;55(1):201-11.

73. Jang, Y.; Choi, W.T.; Johnson, C.T.; García, A.J.; Singh, P.M.; Breedveld, V.; Hess, D.W.; Champion, J.A. Inhibition of bacterial adhesion on nanotextured stainless steel 316L by electrochemical etching. *ACS Biomater. Sci. Eng.* 2018 Jan 8;4(1):90-7.

74. Ismail, R.; Aviat, F.; Michel, V.; Le Bayon, I.; Gay-Perret, P.; Kutnik, M.; Federighi, M. Methods for recovering microorganisms from solid surfaces used in the food industry: a review of the literature. *Int. J. Environ. Res. Public Health.* 2013 Nov 14;10(11):6169-83.

75. Owens, D.K.; Wendt, R.C. Estimation of the surface free energy of polymers. *J. Appl. Polym. Sci.* 1969 May 14;13(8):1741-7.

76. Wenzel, R.N. Surface roughness and contact angle. *J. Phys. Colloid Chem.* 1949 Sep 1;53(9):1466-7.

77. Cassie, A.B.D.; Baxter, S. Wettability of porous surfaces. *Trans. Faraday Soc.* 1944 Jun 19; 40:546-51.

78. Hamadi, F.; Latrache, H.; Zahir, H.; Elghmari, A.; Timinouni, M.; Ellouali, M. The relation between *Escherichia coli* surface functional groups' composition and their physicochemical properties. *Braz. J. Microbiol.* 2008 Apr 14;39(1):10-5.

국문초록

부직포의 젖음성과 기공 특성이 박테리아 부착성에 미치는 영향

HEMMATIAN TAHMINEH
의류학과
서울대학교 대학원

섬유상에 부착된 박테리아는 냄새를 유발하고 전염병 확산 매개체로 작용을 하는 등 위생 상의 문제를 일으키므로 박테리아의 부착을 억제하기 위한 연구가 다수 진행되고 있다. 본 연구의 목표는 부직포 직물의 표면 특성 및 직물 기공 구조에 따른 박테리아의 부착성을 조사하는 것이다.

첫 번째 단계로, 섬유상에 부착된 박테리아의 정량을 위해 INT(iodonitrotetrazolium) colorimetric bacteria assay를 이용한 박테리아 비색 검출을 수행했다. 이어서 연구의 두 번째 단계에서는 부직포 직물의 젖음성, 기공도(%), 기공 부피 및 기공 크기 분포를 포함한 섬유 물리화학적 특성이 박테리아 부착성에 어떻게 영향을 미치는지 조사하였다. 모델 박테리아로 그람 음성 간균인 대장균(*E.*

coli)과 그람 양성 구균인 황색 포도상구균(*S. aureus*)을 사용했다.

표면의 젖음성은 박테리아 부착성에 영향을 미치는 주요 요인으로 조사되었으며, 친수성 표면에서 박테리아 부착량이 높게 나타났는데, 이는 젖음성이 높은 표면에서 박테리아와의 접촉면적이 크기 때문으로 사료된다. 기공도(%) 자체보다는 기공이 차지하는 절대적인 부피와 기공의 크기가 박테리아 부착에 더 큰 영향을 미치는 것으로 나타났다. 섬유의 solidity가 높고 기공크기가 박테리아보다 작은 고밀도 조직에서 박테리아의 침입 가능성이 낮아져서 부착성이 낮았으며, 기공크기가 매우 큰 부직포의 경우에도 직물에 침투한 박테리아가 잘 빠져나가기 때문에 부착성이 비교적 낮았다. 본 연구의 결과는 섬유의 방오성과 항균성을 증진시키는데 활용될 수 있을 것으로 기대한다.

주요어 : 박테리아 부착, 젖음성, 표면특성, 기공, electrospun web, morphology; pore; plasma treatment; *Staphylococcus aureus*; *Escherichia coli*

학 번 : 2018-28019